COMPUTATION OF DRAIN AND SUBSTRATE CURRENTS IN ULTRA-SHORT-CHANNEL NMOSFET'S USING THE HYDRODYNAMIC MODEL

Khalid Rahmat Jacob White Dimitri A. Antoniadis
Department of Electrical Engineering and Computer Science
Massachusetts Institute of Technology
Cambridge, MA 02139

ABSTRACT

The goal of this work was to develop a robust and efficient numerical solution of the hydrodynamic model, which solves the energy balance equation, and to compare predictions of this model, using one set of parameters, with experimental nMOSFET characteristics for a range of channel lengths down to ultra short channels. The substrate current was calculated by direct integration of the energy distribution function to obtain the number of high energy electrons.

INTRODUCTION

In this paper we use the basic formulation of [1] and keep the full energy balance equation but neglect the nonlinear convective term in the momentum conservation equation. We then modify the discretization of the energy balance equation to take into account explicitly the variation of the thermal conductivity with carrier concentration. This scheme is shown to be numerically more stable than the schemes proposed in [2] and [3], which produce instabilities when used with coarse meshes. We have implemented the hydrodynamic model for one carrier in steady state in a two-dimensional device simulator, and the simulated device characteristics match well with the experimental data for MOSFET's with channel lengths from $0.16\,\mu$m to $0.90\,\mu$m. This was achieved by using one set of model parameters for all channel lengths and with the simulator calibrated at $0.90\,\mu$m.

We also present the results of a simple method to calculate the substrate current based on computed electron temperatures. The method predicts quite well the experimentally observed substrate current for MOSFET's over a range of channel lengths and transistor biases. As the substrate current is a sensitive measure of the hot carrier population, accurate prediction of the substrate current provides an independent check on the validity of the computed solution to the energy equation.

THE HYDRODYNAMIC MODEL

The momentum and energy conservation laws for electron transport can be written in the form [1]:

$$\mathbf{J}_n - \frac{\tau_n}{q}\left(\mathbf{J}_n \cdot \nabla\right)\left(\frac{\mathbf{J}_n}{n}\right) = qD_n\nabla n - q\mu_n n\nabla\left(\psi - \frac{k_BT}{q}\right) \quad (1)$$

$$\nabla\cdot\left[-\kappa\nabla T - \frac{\mathbf{J}_n}{q}(k_BT + w)\right] = \mathbf{E}\cdot\mathbf{J}_n - n\left(\frac{w - w_0}{\tau_w}\right) - wU. \quad (2)$$

In the above equations, n is the electron concentration, $\mathbf{J}_n$ is the electron current and w is the electron energy which is given by

$$w = \frac{1}{2}m_n^* v_n^2 + \frac{3}{2}k_BT \quad (3)$$

These along with current continuity and Poisson's equation form the hydrodynamic model. Our simulations were performed with the mobility and thermal conductivity model in [4].

DISCRETIZATION SCHEME

In the discretization scheme used in [3], which is an extension of the work in [2], the problem is cast in terms of an energy flow density, S, defined by

$$\mathbf{S} = -\kappa\nabla T - \left(\frac{5}{2}k_BT\right)\frac{\mathbf{J}_n}{q}. \quad (4)$$

Thus the energy equation can be written as

$$\nabla\cdot\mathbf{S} = \nabla\cdot\left(-q\psi + \frac{m_n^*|\mathbf{J}_n|^2}{2q^2n^2}\right)\frac{\mathbf{J}_n}{q} + (q\psi - w)U - n\frac{w - w_0}{\tau_w}. \quad (5)$$

One advantage of this formulation is that a Scharfetter-Gummel or exponentially-fit discretization scheme can be applied. This can be seen by projecting S onto an edge between nodes i and j,

$$S_{ij} = -\kappa\frac{dT}{dx_{ij}} - \frac{5}{2}\frac{k_BT}{q}J_{ij}. \quad (6)$$

Treating S_{ij}, J_{ij} and κ as constant along the edge, (6) can be integrated analytically to obtain:

$$S_{ij} = -\frac{\kappa_{ij}}{d_{ij}}\left[B(\omega_{ij})T_j - B(-\omega_{ij})T_i\right], \quad (7)$$

CH3075-9/91/0000-0115 $1.00 © 1991 IEEE

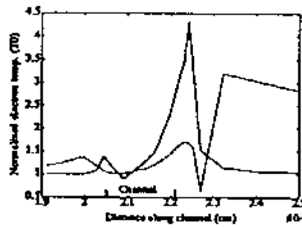

Figure 1: Simulated electron temperature for a MOSFET along the device at two different depths from the oxide interface with unstable discretization.

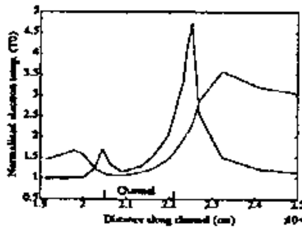

Figure 2: Simulated electron temperature for a MOSFET along the device at two different depths from the oxide interface with stable discretization.

where

$$\omega_{ij} = -\frac{5}{2} k_B \frac{J_{ij}}{q} \frac{d_{ij}}{\kappa_{ij}}, \qquad (8)$$

and $B(x) = \frac{x}{e^x - 1}$ is the Bernoulli function, κ_{ij} is an average thermal conductivity between the two nodes, and d_{ij} is the distance between nodes i and j.

Temperature Instabilities

The above discretization technique was implemented in a two-dimensional finite-box based device simulator and used to simulate a short channel MOSFET. To solve the nonlinear algebraic problem generated by the discretization, a Newton's method was used, combined with a sparse Gaussian elimination used to solve for the Newton updates. We observed that the temperatures computed using a coarse rectangular mesh with the discretization method described above exhibited numerical instabilities in certain regions of the device. In particular the computed temperatures oscillated in space, occasionally dipping *below* the lattice temperature. An example of this anomalous behavior is shown in Fig. 1.

The source of this numerical instability is that the discretization of the energy equation in (7) and (8) inappropriately assumes that the thermal conductivity is a constant. To see why such an approximation leads to coarse-grid instability, consider computing the divergence of (4) assuming $\mathbf{J}_n$, but *not* κ, is constant. The result is

$$\nabla \cdot \mathbf{S} = -\kappa \nabla^2 T - \left(\nabla \kappa + \left(\frac{5}{2} k_B \right) \frac{\mathbf{J}_n}{q} \right) \nabla T. \qquad (9)$$

To be stable for coarse grids, a method for discretizing (9) must *upwind* the ∇T term, that is discretize ∇T in the upwind direction given by the sign of

$$\left(\nabla \kappa + \left(\frac{5}{2} k_B \right) \frac{\mathbf{J}_n}{q} \right). \qquad (10)$$

Equation (8) does not include the $\nabla \kappa$ term, and therefore the resulting Scharfetter-Gummel scheme will not upwind correctly unless the $\nabla \kappa$ term can be ignored. This is not the case, if we write the thermal conductivity as

$$\kappa = \left(\frac{5}{2} + c \right) k_B D_{n0} n \qquad (11)$$

and substitute this relation in (10) to yield

$$\left(\frac{5}{2} k_B \right) \left(\left(1 + \frac{2}{5} c \right) D_{n0} \nabla n + \frac{\mathbf{J}_n}{q} \right) \nabla T. \qquad (12)$$

Clearly, $\left(1 + \frac{2}{5}c\right) D_{n0} \nabla n$ and $\frac{\mathbf{J}_n}{q}$ will be comparable when diffusion contributes significantly to current flow. In particular, this implies that the ∇T term in (9) may not be discretized in the upwind direction when ∇n is large. Our numerical experiments verify this, as the temperatures computed with the above approach oscillate in device regions where the electron concentration gradients are large.

Modified Energy Discretization

In this section, we develop a better stabilized discretization scheme for the energy equation. The convective term in (1)

$$\frac{\tau_n}{q} \left(\mathbf{J}_n \cdot \nabla \right) \left(\frac{\mathbf{J}_n}{n} \right) \qquad (13)$$

is explicitly neglected, which makes it possible to substitute the expressions for the thermal conductivity, κ, and electron current density, $\mathbf{J}_n$, into the energy equation as suggested by [5]. The justification for neglecting the convective term is that in MOSFETs where current flow is by majority carriers, this term is generally small compared to $\mathbf{J}_n$ in regions where the electron concentration is large.

Neglecting the convective term, (1) becomes

$$\mathbf{J}_n \simeq q \frac{k_B T_0}{q} \mu_n \left[r \nabla n + n \nabla (r - u) \right] \qquad (14)$$

where $r = \frac{T}{T_0}$ is the electron temperature normalized by the lattice temperature and u is the normalized electostatic potential given by $u = \frac{q}{k_B T_0} \psi$. Note (14) is identical to (6.4) in [2], once the convective term is neglected. The termperature dependence of the mobility model can be included explicitly into the current equation, as in

$$\mathbf{J}_n = q \frac{D_{n0}}{r} \left[r \nabla n + n \nabla (r - u) \right]. \qquad (15)$$

Substituting both the expression for the current (15) and the thermal conductivity (11) into the energy flux equation yields

$$\mathbf{S} = -\frac{5}{2}k_B T_0 D_{n0}\left[r\nabla n + n\left((2+\frac{2}{5}c)\nabla r - \nabla u\right)\right] \qquad (16)$$

The above expression for S has the same form as that for $\mathbf{J}_n$ (15) but with a different coefficient in front of the ∇r term. Hence, the Scharfetter-Gummel method can be just as easily applied to this equation as to the current equation, with presumably equal success. Just as in the equation for $\mathbf{J}_n$, we have assumed that the electron temperature and electrostatic potential vary linearly between the two nodes. This assumption more naturally captures the physical variation of these variables, as it is the electron concentration which needs to be "exponentially fitted" rather than the electron temperature. It should be pointed out though this approach leads to inconsistent forms for the electron concentration obtained from (15) and (17) but this inconsistency disappears as the grid size shrinks.

The discretization of the right hand side of (5) poses no special difficulties, and is handled in a conventional manner.

Using the above discretization scheme with the same mesh spacing and biases as used in Fig. 1, the solution shown in Fig. 2 does not display instability.

SIMULATION RESULTS

In this section we compare the results obtained from our two-dimensional simulator for devices with effective channel lengths from 0.16 μm to 0.90 μm with experimental data from [8]. Gate oxide thickness for these devices was 52 Å, the junction depth is about 0.09 μm and the device width is 10 μm for all the simulated MOSFET's. One set of parameters was used for all devices and no fine tuning of the parameters in the device models was performed with the exception of adding a series resistance to the source and drain of the simulator. Note that a constant series resistance was used for all devices.

Substrate Current Calculation

As the substrate current in MOS transistors at high drain biases is primarily due to impact ionization, a standard model for substrate current is to assume that it is proportional to the number of electrons above a threshold energy. That is,

$$I_{sub} = C_{sub}W\int_0^{L_x}\int_0^{L_y} dx\; dy\; n(x,y)\int_{\varepsilon_{Thresh}}^{\infty} d\varepsilon\, F(\varepsilon, T(x,y)). \qquad (17)$$

where ε, ε_{Thresh} are the electron and threshold energies respectively; $F(\varepsilon, T)$ is the product of the electron energy distribution and the density of states as a function of temperature; L_x, L_y, W are the device length, height, and width respectively; and C_{sub} is a proportionality constant. Note that w which is the average electron energy is distinct from ε which is a dummy variable.

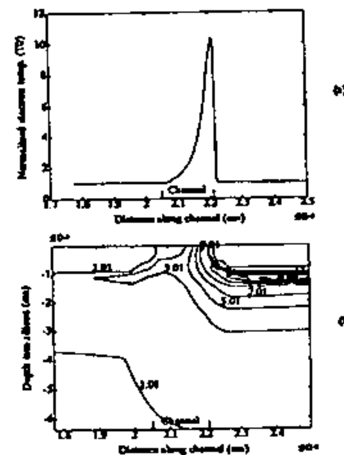

Figure 3: Electron temperature normalized to the lattice temperature in the 0.16 μm MOSFET. (a) at the silicon-oxide interface and (b) contour plot in the channel region.

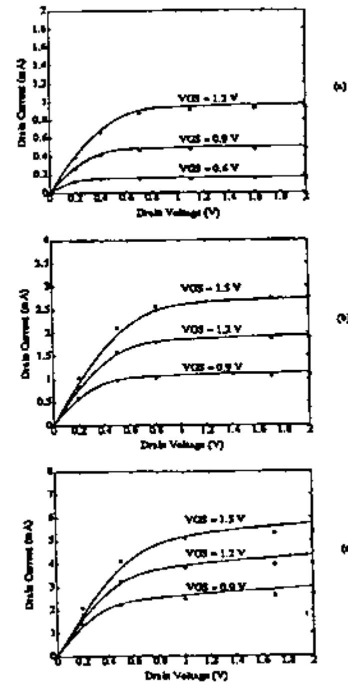

Figure 4: Experimental (solid) and simulated (o) drain current for three MOSFET's with channel lengths of (a) 0.90 μm (b) 0.40 μm (c) 0.16 μm.

For the two-dimensional simulations discussed in this paper, uniformity along the width is implicitly assumed, and therefore integration with respect to the width is replaced by multiplication.

Under high field conditions, it is well known that the actual electron energy distribution is substantially different from Maxwellian. Recent Monte-Carlo studies [6], [7] suggest that the tail of the distribution function decays much faster than an exponential dependence. In [6], it is proposed that a more accurate model would be to use a cubic energy dependence in the exponent. This result was derived analytically using non-parabolic bands which, of course, also changes the density of states. Thus, in our notation, this leads to

$$F(\varepsilon, T) = C_{dist}(T)\varepsilon^{1.25} \exp\left(-\chi \frac{\varepsilon^3}{T^{1.5}}\right) \tag{18}$$

where

$$C_{dist}(T) = \frac{1}{\int_0^\infty \varepsilon^{1.25} \exp\left(-\chi \frac{\varepsilon^3}{T^{1.5}}\right)}. \tag{19}$$

The constant χ is chosen during calibration, and is selected so that the same threshold energy can be used for comparisons between the Maxwellian distribution and (18).

The above substrate current model has only two free parameters, the threshold energy and C_{sub}. Calibration was performed by insuring a good fit to measured substrate current data for a $0.4\,\mu$m channel-length device over a range of biases. For our data, the resulting calibration threshold energy was 2.1 eV. These same threshold energy and proportionality constants were used for all the computed results presented below.

Fig. 5 shows the simulated and measured substrate currents at different gate biases for both devices using the cubic distribution function. Generation-recombination is ignored in our simulator so only a comparison with the hot carrier part of the substrate current is appropriate.

The above approach is similar to that presented in [3].

CONCLUSION

The results in this paper demonstrate that the hydrodynamic model can be used successfully to simulate silicon MOSFET's with channel lengths as short as $0.16\,\mu$m. Equally important is the fact that one set of parameters was used to simulate devices with channel lengths varying from $0.90\,\mu$m down to $0.16\,\mu$m and all the parameter values used were physically justifiable. We have also shown the importance of using a stable discretization method in the energy balance equation to avoid spurious numerical results. Finally, an approach to computing the substrate currents by the direct integration of the energy distribution function yielded a simple, but reasonably accurate, method.

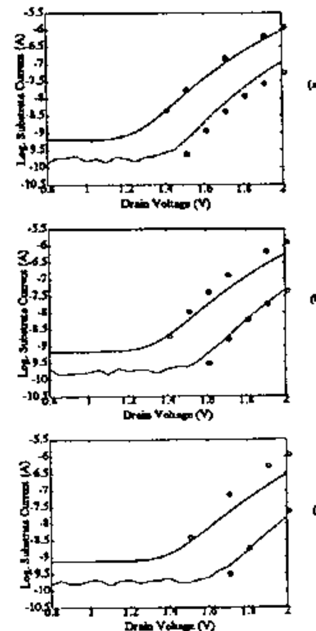

Figure 5: Simulated (o) and measured substrate current for the $0.16\,\mu$m (solid) and $0.40\,\mu$m (dash) devices using the cubic distribution function. (a) $V_{GS} = 0.9V$; (b) $V_{GS} = 1.2V$; (c) $V_{GS} = 1.5V$.

Acknowledgement

The authors would like to thank J. Jacobs for his help on mobility models and calibration techniques, Dr. G. Shahidi for providing the experimental data and Dr. F. Odeh for many valuable discussions.

References

[1] M. Rudan et al., *COMPEL*, vol. 5, pp. 149-183, 1986.

[2] A. Forghieri, et al., *IEEE Trans. Computer-Aided Design*, vol. 7, pp. 231-242, 1988.

[3] M. Gnudi et al., Invited Talk, SIAM Meeting, Chicago, July 1990.

[4] G. Baccarani et al., *Solid State Electron.*, vol. 28, 407-416, 1985.

[5] T. W. Tang, *IEEE Trans. Electron Devices*, vol. ED-31, pp. 1912-1914, 1984.

[6] D. Cassi et al., *IEEE Trans. Electron Devices*, vol. ED-37, pp. 1514-1521, 1990.

[7] N. Goldsman et al., *IEEE Electron Device Lett.*, vol. 11, pp. 472-474, 1990.

[8] G. Shahidi et al., *IEEE Electron Device Lett.*, vol. 9, pp. 497-499, 1988.